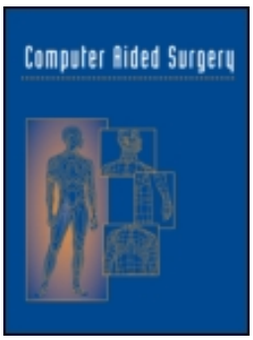

Computer Aided Surgery

ISSN: 1092-9088 (Print) 1097-0150 (Online) Journal homepage: http://www.tandfonline.com/loi/icsu20

Flexible needle steering for percutaneous therapies

Daniel Glozman & Moshe Shoham

To cite this article: Daniel Glozman & Moshe Shoham (2006) Flexible needle steering for percutaneous therapies, Computer Aided Surgery, 11:4, 194-201

To link to this article: http://dx.doi.org/10.3109/10929080600893019

Computer Aided Surgery, July 2006; 11(4): 194–201

informa
healthcare

BIOMEDICAL PAPER

Flexible needle steering for percutaneous therapies

DANIEL GLOZMAN & MOSHE SHOHAM

Mechanical Engineering Department, Technion – Israel Institute of Technology, Haifa, Israel

(Received 6 July 2005; accepted 25 March 2006)

Abstract
Objective: A robotic system is presented for flexible needle steering and control in soft tissue.
Materials and Methods: Flexible needle insertion into a deformable tissue is modeled as a linear beam supported by virtual springs, where the stiffness coefficients of the springs can vary along the needle. Using this simplified model, the forward and inverse kinematics of the needle are solved analytically, thus enabling both path planning and path correction in real time. Given target and obstacle locations, the computer calculates the needle tip trajectory that will avoid the obstacle and hit the target. Using the inverse kinematics algorithm, the corresponding needle base maneuver needed to follow this trajectory is calculated.
Results: It is demonstrated that the needle tip path is not unique and can be optimized to minimize lateral pressure of the needle body on the tissue. Needle steering, i.e., the needle base movements that steer the needle tip, is not intuitive. Therefore, the needle insertion procedure is best performed by a robot. The model was verified experimentally on muscle and liver tissues by robotically assisted insertion of a flexible spinal needle. During insertion, the position and shape of the needle were recorded by X-ray.
Conclusions: This study demonstrates the ability to curve a flexible needle by its base motion in order to achieve a planned tip trajectory.

Keywords: *Needle insertion, percutaneous therapy, virtual spring, inverse kinematics, robotic assistance*

Introduction

The trend in contemporary medicine is towards less invasive and more localized therapy. Many routine treatments employed in modern clinical practice involve percutaneous insertion of needles and catheters for biopsy and drug delivery. The aim of a needle insertion procedure is to place the tip of an appropriate needle safely and accurately in the lesion, organ or vessel. Examples of treatments requiring needle insertions include vaccinations, blood/fluid sampling, regional anesthesia, tissue biopsy, catheter insertion, cryogenic ablation, electrolytic ablation, brachytherapy, neurosurgery, deep brain stimulation and various minimally invasive surgeries. In general, complications of percutaneous needle insertion are due to poor technique and needle placement [1]. Physicians and surgeons often rely only on kinesthetic feedback from the tool that they correlate with their own mental 3D perception of anatomic structures. However, this method has significant limitations: as the needle penetrates the tissue, the tissue deforms and thus, even when working with straight rigid needles, the target can be missed [2]. To improve needle placement, rigid needles can be maneuvered under image guidance. Furthermore, Alteroviz et al. [3] have proposed a way to predict rigid needle placement error in prostate brachytherapy procedures and to correct for this error by choosing an alternative insertion point. Despite such advances in rigid needle

Correspondence: Daniel Glozman, Medical Robotics Laboratory, Mechanical Engineering Department, Technion – Israel Institute of Technology, Haifa, Israel, 32000. Tel: +972-4-829-5654. E-mail: glozmand@technion.ac.il
Prof. Moshe Shoham, Mechanical Engineering Department, Technion – Israel Institute of Technology, Haifa, Israel, 32000. Tel: +972-4-829-2102. Fax: +972-4-829-5711. E-mail: shoham@technion.ac.il Website: http://robotics.technion.ac.il

ISSN 1092-9088 print/ISSN 1097-0150 online
DOI: 10.1080/10929080600893019

placement, in some cases the problem persists of rigid needles causing excessive, injurious pressure on tissues.

An alternative approach to ensuring the success of percutaneous procedures is to employ thin and flexible needles. There are numerous advantages to using such needles. According to retrospective studies that examined the relationship between post-biopsy behavior and biopsy needle diameter, less serious complications occur with fine (<1 mm) biopsy needles than with standard coarse needles [4]. Furthermore, thinner needles cause less damage and reduce the chance of Post Dural Puncture Headache (PDPH) appearing after spinal anesthesia; indeed, the relative risk of PDPH decreases with reduction in needle diameter [5]. Moreover, flexible needles facilitate curved trajectories that may be desirable in order to avoid sensitive tissues, such as bone or blood vessels, lying between the feasible entry points and potential targets. However, a major disadvantage to using thin flexible needles is that they are very difficult to control. They have non-minimum phase behavior and do not lend themselves to intuitive (human) control. Solving this problem of control requires development of a computerized robotic system that can plan and perform insertions of thin flexible needles. Creation of such a system represents a challenge for mechanical engineers and roboticists, but is nevertheless an urgent therapeutic goal as it will reduce morbidity and patient suffering following percutaneous procedures.

Devising a method to predict flexible needle motion was first addressed by DiMaio and Salcudean [6]. To solve the inverse kinematics of the needle, the authors used iterative numerical computing of the Jacobian-modeled movement exhibited by a flexible needle. The solution requires nine independent computations for devising the Jacobian elements that account for the two-dimensional (2D) finite element mesh of the tissue and the iterative nonlinear flexion of a beam. A limitation of this work is that, due to the computational complexity, it does not allow for real-time simulation and control of the needle path. An active, flexible steering system using shape memory alloys has been suggested for steering a catheter [7]. However, such a system is not suitable for thin needle navigation because of its size limitations. Several groups have focused on calculating the effects of needle bending. Kataoka et al. investigated needle deflection due to the bevel of the tip during linear needle insertion and expressed the deflection as a function of the driving force [8]. O'Leary et al. demonstrated experimentally that needle bending forces are significantly affected by the presence of a bevel tip [9]. Ebrahimi et al. generated needle bending by incorporating a pre-bent stylus inside a straight canula [10]. Such studies have led to the realization that bevel-tip needles can be steered by taking advantage of needle bending and by exploiting the asymmetric force applied by the needle tip to the tissue. This insight encouraged recent work aimed at steering a highly flexible needle through firm tissue by formulating its motion as a nonholonomic kinematics problem [11–13]. It is notable that the effect of the beveled tip decreases with reduction in needle diameter, as the lateral force is proportional to the area of the tip.

The present investigation describes an algorithm that allows fast path planning and real-time tracking of a flexible needle insertion procedure. The aim of this work is the creation of an image-based system for automatic flexible needle insertion and obstacle avoidance.

Materials and methods

Virtual springs model

In this investigation, modeling the movements of a flexible needle is based on the assumption of quasi-static motion; the needle is in an equilibrium state at each step. It is known that needle deflection due to interactions with biologic soft tissue is nonlinear with strain. However, the work of Simone et al. implies that it is reasonable to assume a linear lateral force response for small displacements [14, 15]. The tissue forces on the needle are modeled as a combination of lateral virtual springs distributed along the needle curve plus friction forces tangent to the needle. Since the tissue elastic modulus changes as a function of strain, we update the coefficients of the virtual springs according to the strain-dependent dynamic elastic modulus and linearize the system at each step. The concept is illustrated in Figure 1.

As the shape of the needle changes, the location and orientation of the virtual springs change accordingly. The linearized system model yields the shape of the needle at each step. There is no physical meaning to the free length of the virtual springs. The only important parameter of a spring is the local stiffness coefficient that expresses the force of the tissue on the needle as a function of local displacement. The stiffness coefficients of the virtual springs are determined experimentally or by using preoperative images assuming empiric stiffness values of tissues and organs [15].

The linearized system solution. Assuming small displacements, the needle is approximated by a linear beam subjected to point forces, as shown in Figure 2. With appropriate spacing of elements, it can approximate a flexible beam according to the elastic foundation model.

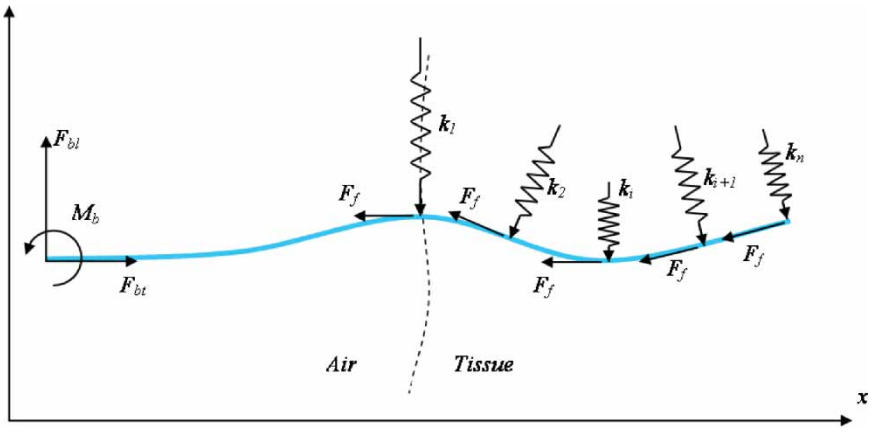

Figure 1. Virtual springs model. The interaction of the tissue with the needle is modeled by distributed virtual springs. [Color version available online.]

At each joint, the force applied by a virtual spring is proportional to the displacement of the spring from its initial position:

$$F_i = k_i(w_i - w_{0i}) \tag{1}$$

where k_i is the virtual spring coefficient, w_i the displacement at point i, and w_{0i} the position of freed spring i.

As the forces are a function of the deflection, the needle movement cannot be modeled by treating the beam as one element. Therefore, the beam is split into a number of elements, so that each beam element is subjected to two neighboring forces. Thus, the first element is the part of the needle outside of the tissue, and the rest of the elements are distributed along the inner part according to the level of discretization. Each element behaves as a linear beam subjected to shearing forces at its borders. The displacement of each element is given by a third degree polynomial. We adopt the nodal degrees of freedom from finite elements theory, in which the coordinates are specifically identified with a single nodal point and represent a displacement or rotation, having clear physical interpretation. The displacement $y(x)$ has the form of

$$y(x) = N_1\phi_1 + N_2\phi_2 + N_3\phi_3 + N_4\phi_4 \tag{2}$$

where N_1, N_3 are the coordinates and N_2, N_4 are the slopes at $x = 0$ and $x = l$ of an element, respectively. ϕ_i are the shape functions of third degree.

Substituting boundary conditions as displacement and slope at the base and tip of the needle, the result is $4 \times n$ equations: 2 at each side and 4 for each internal node, which yields the global matrix equation

$$[K]\bar{N} = \bar{Q} \tag{3}$$

where K is the matrix of coefficients of $N_{i,j}$-elements degrees of freedom, and N is the vector of $N_{i,j}$, where i is the element number and j is the degree of freedom of element i.

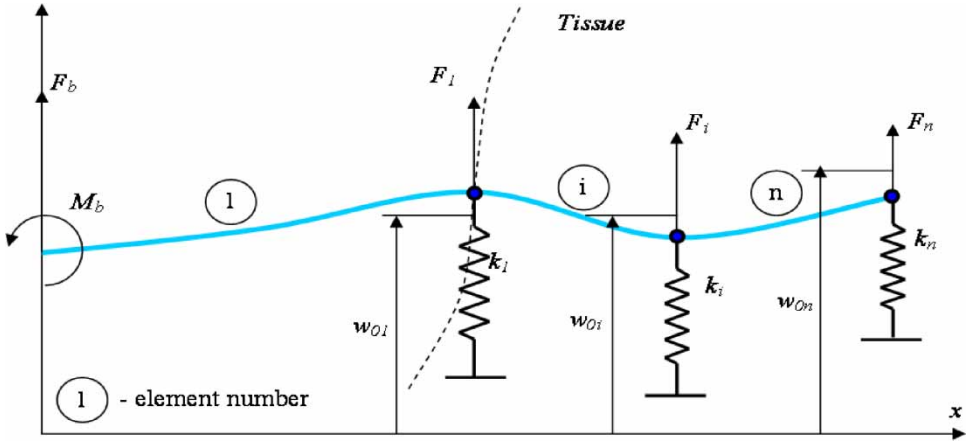

Figure 2. Linear system model. A flexible beam subjected to a number of virtual springs. [Color version available online.]

Forward kinematics. The above solution solves for the translation and rotation of the needle taking into account 2 degrees of freedom (DOF) of the needle base: vertical translation y and slope θ. Applying axial translation, along the x-direction, to the non-compressible needle means that the part of the needle outside the tissue is shortened by the amount of the translation Δx, while an additional element of length Δx is added to the last element of the needle. Assuming that the last $(n+1)$ element is relatively small, and that the forces on it create negligible moments, its shape is taken as a straight line with the slope of the previous element.

In summary, given the translation and a rotation of the needle base, we are now able to calculate the 3-DOF translation and rotation of the needle tip, thus completing the forward kinematics solution.

Inverse kinematics. In an actual needle insertion problem, there is a need to hit the target with the tip while at the same time avoiding possible organ obstacles. Therefore, a particular trajectory is desired for the tip of the needle and it is the manipulation to be performed at the needle base that is calculated. This is an inverse kinematics problem, i.e., given the position and orientation of the tip trajectory, the translation and orientation of the needle base is derived.

Let us expand the matrix in equation (3):

$$\begin{bmatrix} 1 & 0 & \dots & 0 & 0 \\ 0 & -1 & \dots & 0 & 0 \\ & \tilde{K}_{21} & & \tilde{K}_{22} & \end{bmatrix} \begin{pmatrix} N_{11} \\ N_{12} \\ \vdots \\ N_{n3} \\ N_{n4} \end{pmatrix} = \begin{pmatrix} Y \\ \theta \\ \vdots \\ \vdots \\ \vdots \end{pmatrix} \tag{4}$$

Given the base translation Y and rotation θ, one can solve for $N_{i,j}$. Note that the last two elements of vector N are the translation and rotation of the tip. In the inverse kinematics problem, the translation and rotation of the tip $-N_{n3}$ and N_{n4}–are known and the unknowns are the translation and rotation of the base – Y and θ or N_{11} and N_{12}. As in the last two equations the two variables are known, one can write equation (4) as:

$$\begin{aligned} \left[\tilde{K}_{21}\right]\tilde{\tilde{N}} &= \tilde{\tilde{Q}} - \tilde{K}_{22}\begin{pmatrix} N_{n3} \\ N_{n4} \end{pmatrix} \\ Y &= N_{11} \\ \theta &= N_{12} \end{aligned} \tag{5}$$

where $\tilde{\tilde{N}}$, $\tilde{\tilde{Q}}$ are the original vectors $\bar{N}$,$\bar{Q}$ without the last two elements. $\tilde{K}_{21}$ is an $(n-2) \times (n-2)$ matrix, and equation (5) can be solved for $\bar{N}$ and therefore for Y and θ, which is the solution of the inverse kinematics.

Path planning. Planning of a linear insertion path is trivial. The main challenge is avoiding obstacles while applying minimal lateral pressure to the tissue. In the presence of obstacles, the optimal needle path requires minimal curvature of the needle. The path planning problem thus reduces to finding the shortest curve that connects the target to the needle insertion point, which avoids the obstacle while maintaining minimal needle curvature.

As every step is dependent on the history of the insertion, full simulation of the needle insertion is required. Figure 3 shows several solutions of the path planning where the target point is reached with different tip inclinations.

As the orientation of the tip is of less importance in biopsy, one can choose from the infinite solutions the one that applies minimal pressure to the tissue. This is achieved by minimizing the sum of squares of the virtual springs deflections, the sum of which is given by S:

$$S = \min \sum_{i=1}^{n} (w_i^2 + \theta_i^2) = \min \sum_{i=1}^{n} \sum_{j=1}^{4} N_{ij}^2 \tag{6}$$

Differentiating equation (6) with respect to θ_t and equal to zero one obtains:

$$\frac{dS}{d\theta_t} = \sum_{i=1}^{n} \sum_{j=1}^{4} 2N_{ij} \frac{dN_{ij}}{d\theta_t} = 0 \tag{7}$$

Equation (7) is then substituted into equation (4) for of the slope of the last element N_{n4}.

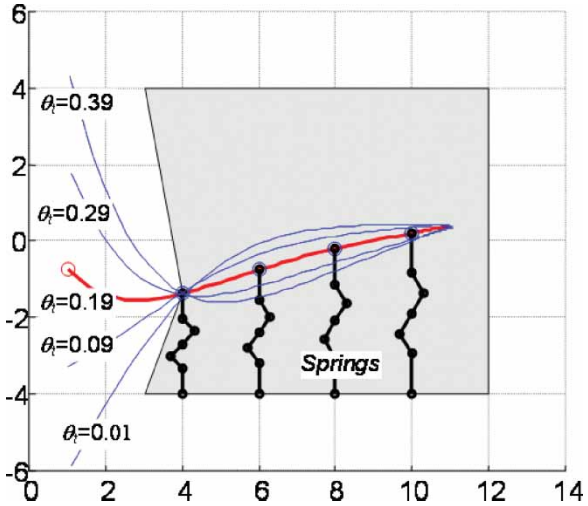

Figure 3. Several needle path solutions for the same tip position with different tip inclinations. [Color version available online.]

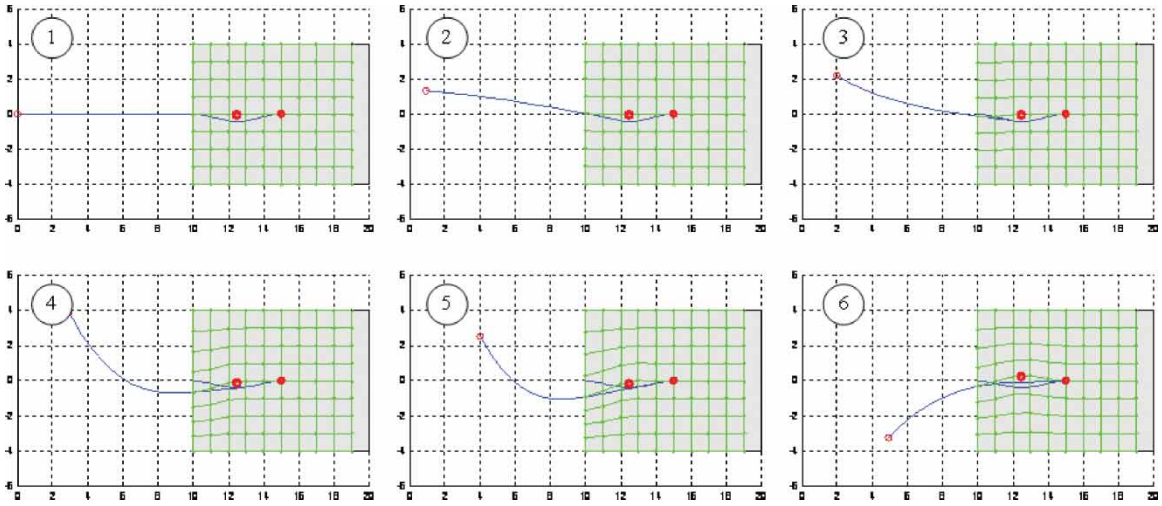

Figure 4. Needle insertion simulation for tip orientation tangent to the path. [Color version available online.]

Needle insertion simulation

Simulations of the needle insertion procedure were carried out. The motion of the needle base induces the needle tip to execute a sine wave path in order to avoid an obstacle in the tissue. In Figures 4 and 5, the left red circle represents an obstacle and the right one is the target.

As the needle penetrates deeper into the tissue, additional virtual springs are introduced and are shown, for simplicity, as a compressible mesh below and above the needle. The needle trajectory is shown for two cases: one where the tip is forced to be tangent to the tip trajectory (Figure 4), and another where the trajectory is optimized for minimal lateral tissue pressure (Figure 5). The simulation starts with one element beam of length 100 mm at step 1. After advancement of 10 mm into the tissue, the element is subdivided, adding a new element of 10 mm and a virtual spring at the tip of the needle. This is repeated such that at the 6^{th} step there are 6 elements and 6 virtual springs.

Results

Two metal pieces were inserted into animal tissue, one as the target and the other as the obstacle. A robot manipulating a needle was then programmed to follow a path, computed using the above algorithm, to avoid the obstacle and hit the target.

The experiment was conducted on chicken breast muscle and animal liver using the RSPR parallel robot [16] shown in Figure 6. The needle is connected to the robot through an ATI Nano17 6-DOF force sensor, and is a spinal 22G × 90 mm type with an outer diameter of 0.71 mm. With

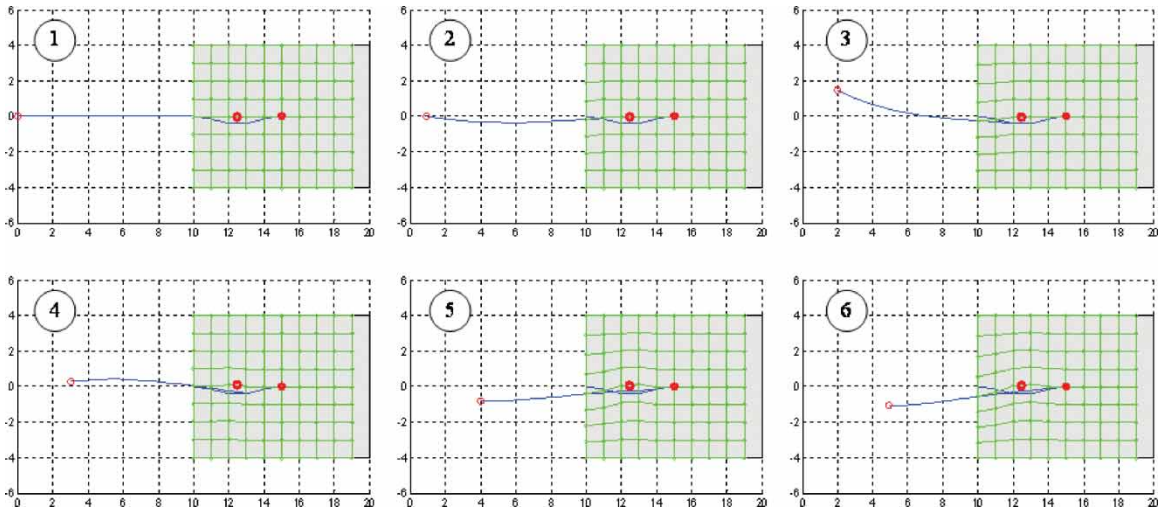

Figure 5. Needle insertion simulation minimizing lateral pressure on the tissue. [Color version available online.]

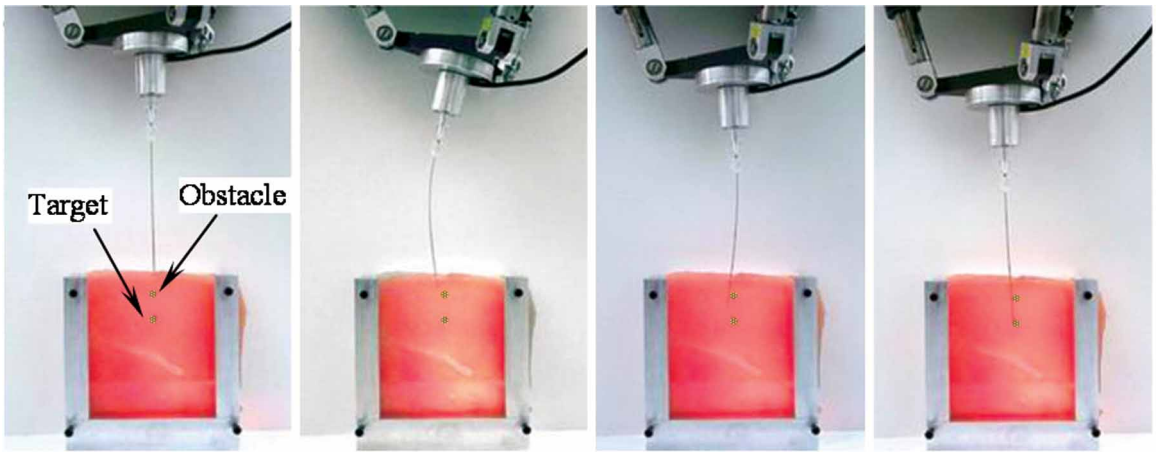

Figure 6. Needle insertion by robot corresponding to simulation steps 1, 3, 4 and 6 (see Figure 5). [Color version available online.]

proper lighting it was possible to see through the tissue and to obtain images of reasonable quality. The tissue is placed in a 100 mm × 100 mm frame and is constrained in one plane between two glass plates. The stiffness coefficient of the virtual springs was evaluated experimentally to be 60 N/m by needle force measurement.

The images corresponding to steps 1, 3, 4 and 6 of the simulation described in the section above (see Figure 5) are shown in Figure 6. As can be seen, the path followed by the needle tip was similar to the simulated path; the tip avoided the obstacle and hit the target.

Experiment with X-ray imaging

The experimental system is shown in Figure 7; it comprises a Siemens C-arm for imaging the RSPR 6-DOF parallel robot, a 6-DOF force sensor, and the spinal needle.

The needle insertion procedure is as follows. First, a single X-ray image of the needle and the tissue is taken (Figure 8a). The user then points to the target and the obstacles on the screen. The computer applies the needle detection algorithm described above to find the position of the needle tip and to calculate the needle insertion path to the target that avoids the obstacles. The detected needle and the planned needle path are then drawn on the image (Figure 8b). Next, the needle insertion path is simulated to check in advance for needle-tissue lateral forces and to confirm the robot's capability to execute the required trajectory. The system is then considered ready to carry out the needle insertion, as shown in Figures 9a and 9b. It can be seen that the needle is bent so that it hits the target while the obstacle is avoided.

It should be noted that the obstacle and target metal balls appears in the images as ellipses because they move during the insertion.

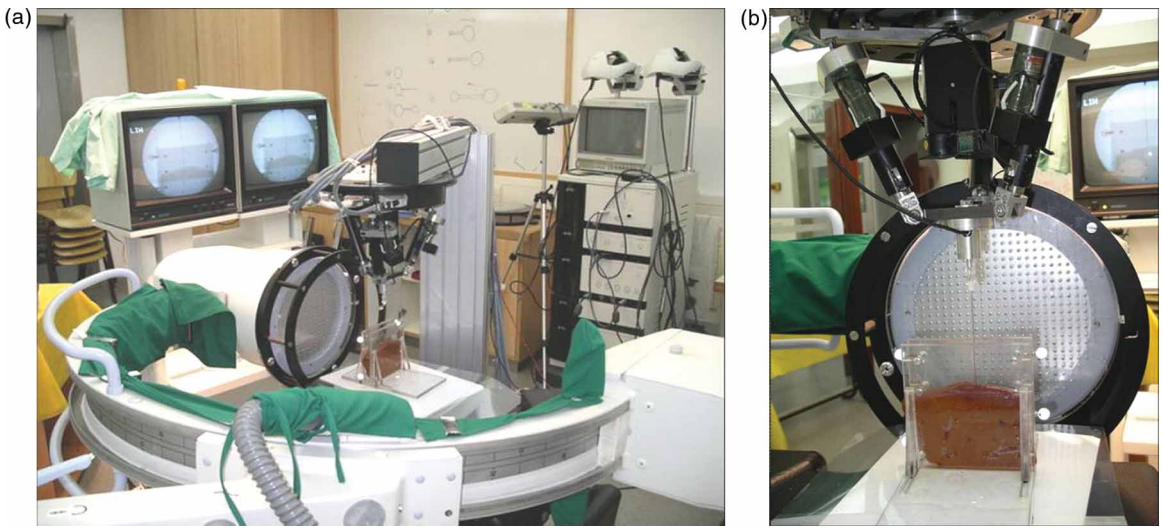

Figure 7. a) Experimental setup with X-ray imaging. b) Spinal needle, force sensor and liver tissue. [Color version available online.]

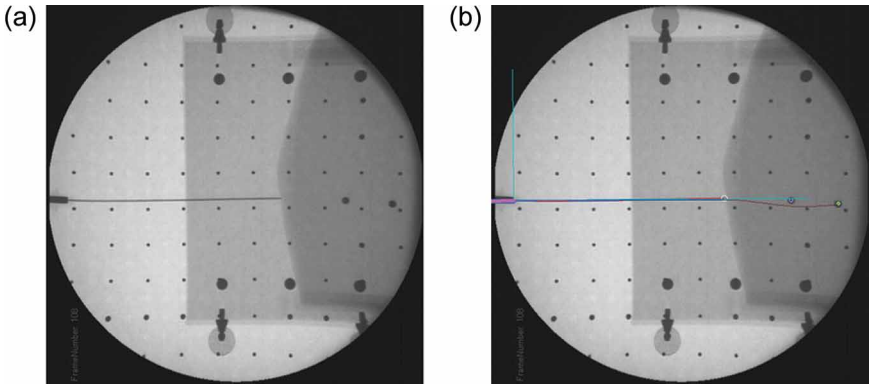

Figure 8. a) Needle and tissue image. b) Detected needle and planned insertion path. [Color version available online.]

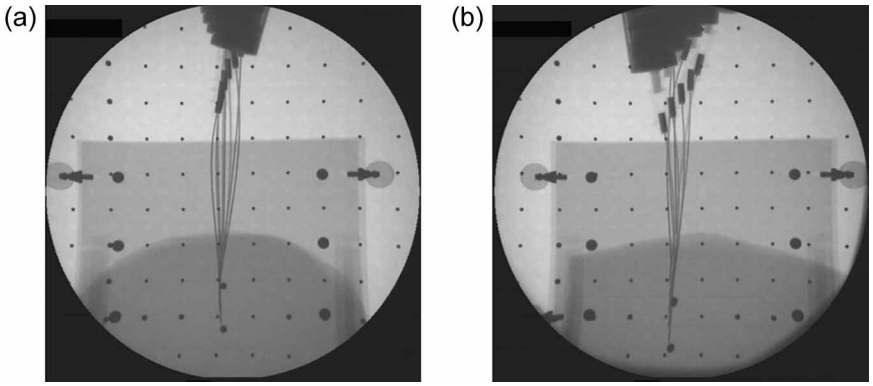

Figure 9. a) Needle insertion in chicken breast. b) Needle insertion in liver.

Discussion

This investigation develops the planar linearized model approximation assuming small deflections to address the flexible needle insertion problem. Using this model, the inverse and forward kinematics of needle insertion are calculated in one step by solving a low-dimensional linear system of equations. Additionally, path planning and its optimization for minimal tissue pressure were developed. It was found that this model can be solved in a closed form for a given needle tip trajectory. Relaxing the requirement that tip orientation be tangent to the path at each point greatly decreases both the needle base stroke and the lateral pressure exerted on the tissue. Using a robot to maneuver the needle base and insert the needle into animal tissues verified the proposed concept. The needle trajectory was similar to the preplanned trajectory, avoiding an obstacle and hitting the target. Imaging the tissue by X-ray enabled an operator to mark on a screen the target and the obstacle from which a computer calculated the needle tip path and the corresponding needle base motion required to accomplish this tip path.

References

1. De Andres J, Reina MA, Lopez-Garcia A. Risks of regional anesthesia: Role of equipment – Needle design, catheters. Proceedings of the VII Annual European Society of Regional Anaesthesia Congress, Geneva, Switzerland, September 1998.
2. DiMaio SP, Salcudean SE. Needle insertion modeling and simulation. IEEE Trans Robotics Automation. Special issue on Medical Robotics, October 2003.
3. Alterovitz R, Pouliot J, Taschereau R, Hsu IJ, Goldberg K. Sensorless planning for medical needle insertion procedures. Proceedings of the 2003 IEEE/RSJ International Conference on Intelligent Robots and Systems (IROS 2003), Las Vegas, NV, October 2003.
4. Grant A, Neuberger J. Guidelines on the use of liver biopsy in clinical practice. Gut 1999;45(Suppl 4): IV1–IV11.
5. Chohan U, Hamdani GA. Post dural puncture headache. J Pak Med Assoc 2003:53(8):359–367.
6. DiMaio SP, Salcudean SE. Needle steering and model-based trajectory planning. In: Ellis RE, Peters TM, editors. Proceedings of the 6th International Conference on Medical Image Computing and Computer–Assisted Intervention (MICCAI 2003), Montreal, Canada, November 2003. Part I. Lecture Notes in Computer Science Vol 2878. Berlin: Springer; 2003. pp 33–40.
7. Mineta T, Mitsui T, Watanabe Y, Kobayashi S, Haga Y, Esashi M. Batch fabricated flat meandering shape memory alloy actuator for active catheter. Sensors and Actuators A: Physical 2001:88;112–120.

8. Kataoka H, Washio T, Audette M, Mizuhara K. A model for relations between needle deflection, force, and thickness on needle penetration. In: Niessen WJ, Viergever MA, editors. Proceedings of the 4th International Conference on Medical Image Computing and Computer-Assisted Intervention (MICCAI 2001), Utrecht, The Netherlands, October 2001. Lecture Notes in Computer Science Vol 2208. Berlin: Springer; 2001. pp 966–974.
9. O'Leary M, Simone C, Washio T, Yoshinaka K, Okamura A. Robotic needle insertion: Effects of friction and needle geometry. Proceedings of the IEEE International Conference on Robotics and Automation, 2003 (ICRA '03), Taipei, Taiwan, September 2003. pp 1774–1780.
10. Ebrahimi R, Okzawa S, Rohling R, Salcudean S. Hand-held steerable needle device. In: Ellis RE, Peters TM, editors. Proceedings of the 6th International Conference on Medical Image Computing and Computer–Assisted Intervention (MICCAI 2003), Montreal, Canada, November 2003. Part II. Lecture Notes in Computer Science Vol 2879. Berlin: Springer; 2003. pp 223–230.
11. Park W, Kim JS, Cowan YZ, Okamura AM, Chirikjian GS. Diffusion–based motion planning for a nonholonomic flexible needle model. In: Proceedings of the 2005 IEEE International Conference on Robotics and Automation, Barcelona, Spain, April 2005.
12. Alterovitz R, Goldberg K. Planning for steerable bevel–tip needle insertion through 2D soft tissue with obstacles. In: Proceedings of the 2005 IEEE International Conference on Robotics and Automation, Barcelona, Spain, April 2005.
13. Webster RJ III, Memisevic J, Okamura AM. Design considerations for robotic needle steering. In: Proceedings of the 2005 IEEE International Conference on Robotics and Automation, Barcelona, Spain, April 2005.
14. Simone C, Okamura A. Haptic modeling of needle insertion for robot-assisted percutaneous therapy. In: Proceedings of the IEEE International Conference on Robotics and Automation, 2002 (ICRA '02), Washington, DC, May 2002. pp 2085–2091.
15. Fung YC. Biomechanics: Mechanics Properties of Living tissues. 2nd edition. New York: Springer; 1993. p 277.
16. Simaan N, Glozman D, Shoham M. Design considerations of new six degrees-of-freedom parallel robots. In: Proceedings of the IEEE International Conference on Robotics and Automation, 1998, Leuven, Belgium, May 1998. Vol 2. pp 1327–1333.